Finite element implementation of an elastoplastic-viscoplastic constitutive law for tunnels

Felipe Pinto da Motta Quevedo[1], Denise Bernaud[2], and Samir Maghous[3]

[1]M.S.,Federal University of Rio Grande do Sul/PPGEC, av. Osvaldo Aranha, 99, Zip-Code 90.035-190, Porto Alegre/RS Brazil. Email: motta.quevedo@ufrgs.br

[2]Ph.D.,Federal University of Rio Grande do Sul/PPGEC, av. Osvaldo Aranha, 99, Zip-Code 90.035-190, Porto Alegre/RS Brazil. Email: denise.bernaud@ufrgs.br

[3]Ph.D.,Federal University of Rio Grande do Sul/PPGEC, av. Osvaldo Aranha, 99, Zip-Code 90.035-190, Porto Alegre/RS Brazil. Email: samir.maghous@ufrgs.br

ABSTRACT

The paper presents an efficient numerical integration scheme for coupled elastoplasticity-viscoplastiticy constitutive behavior with internal-state variables standing for irreversible processes. In most quasi-static structural analyses, the solution to boundary value problems involving materials that exhibit time-dependent constitutive behavior proceeds from the equations integration handled at two distinct levels. On the one hand, the first or local level refers to the numerical integration at each Gaussian point of the rate constitutive stress/strain relationships. For a given strain increment, the procedure of local integration is iterated for stresses and associated internal variables until convergence of the algorithm. On the other hand, the second or global level is related to structure equilibrium between internal and external forces achieved by the Newton-Raphson iterative scheme. A review of the elastoplastic and viscoplastic model will be shown, following the coupling between these models. Particular emphasis is given in this contribution to address the first level integration procedure, also referred to as algorithm for stress and internal variable update, considering a general elastoplastic-viscoplastic constitutive behavior. The formulation is described for

semi-implicit Euler schemes. The efficacy of the numerical formulation is assessed by comparison with analytical solution derived for deep tunnel in coupled elastoplasticity-viscoplascitity.

INTRODUCTION

Deep tunnels are those whose deformation field, induced by excavation, does not significantly reaches the surface. The field of strain and stresses around the cavity of deep tunnel depends on several interrelated factors, such as the depth of the tunnel, the geometry of the cross section, the anisotropy of stresses in situ, the heterogeneity of the rock mass, the coupling between the rock mass and the lining during the construction of the tunnel and the mechanical behavior of the rock mass and lining. In general, for both the rock mass and the lining, several developments in literature of the rheological models are found whose parameters are adjusted based on samples tests.

An elastoplastic-viscoplastic constitutive law becomes important when the material behavior can't be describe by the usual models like elastoplasticity or viscoplastic. This problem is characteristic of deep tunnels excavated in clay rockmass as described by Rousset (1988). In these cases plastification around the rockmass, gradual closing of the tunnel section, extrusion of the excavation face and overloading on the lining can develop over the construction time (short term), or even months and years after the construction of the tunnel (long term), which can lead to excessive deformations (Barla et al. 2008), entrapment of the machine (Ramoni and Anagnostou 2010) and damage to the lining. In addition to the present work, elastoplastic-viscoplastic models applied to the problem of deep tunnels can be found in: Rousset (1988), Piepi (1995), Purwodihardjo and Cambou (2003), Kleine (2007), Shafiqu et al. (2008), Debernardi and Barla (2009), Souley et al. (2011), Manh et al. (2015). This work presents a numerical integration scheme for the elastoplastic-viscoplastic constitutive behavior. For that, a brief bibliographical review will be made about each model separately and later its coupling. Finally, the validation of this model will be presented, comparing its numerical solution with the analytical and numerical solution obtained by Piepi (1995) of an excavated tunnel under axisymmetric conditions.

ELASTOPLASTIC CONSTITUTIVE MODEL

For problems with isothermal evolution, quasi-static in small transformations, the elastoplastic constitutive model can be described through the decomposition of the total strain tensor, the flow surface, the plastic flow rule, the hardening-softening law and the conditions of loading-unloading.

Decomposition of the total strain tensor

Considering the hypothesis of small transformations (which includes the hypothesis of small strains) we have that the total strain rate can be decomposed into an elastic and a plastic component:

$$\dot{\boldsymbol{\varepsilon}} = \dot{\boldsymbol{\varepsilon}}^e + \dot{\boldsymbol{\varepsilon}}^p \ . \tag{1}$$

Within the context of deterministic thermodynamic processes, the specific free energy, considering an isothermal evolution, can be decomposed according to:

$$\psi(\boldsymbol{\varepsilon}, \boldsymbol{\varepsilon}^p, \alpha) = \psi^e(\boldsymbol{\varepsilon} - \boldsymbol{\varepsilon}^p) + \psi^p(\alpha) = \psi^e(\boldsymbol{\varepsilon}^e) + \psi^p(\alpha) \ , \tag{2}$$

where α is the set of internal variables (cohesion, friction angle...) related to the hardening-softening phenomenon. From Eq. (2), the following constitutive relationships are obtained:

$$\boldsymbol{\sigma} = \frac{\partial \psi^e}{\partial \boldsymbol{\varepsilon}^e}, \quad q = \frac{\partial \psi^p}{\partial \alpha} \ , \tag{3}$$

where q is the set of thermodynamic forces associated with internal variables (scalar or tensor). From Eq. (1) and Eq. (3) the following constitutive relationship is obtained:

$$\dot{\boldsymbol{\sigma}} = \boldsymbol{D}^{ep} : \dot{\boldsymbol{\varepsilon}} = \boldsymbol{D} : \dot{\boldsymbol{\varepsilon}}^e = \boldsymbol{D} : (\dot{\boldsymbol{\varepsilon}}^e - \dot{\boldsymbol{\varepsilon}}^p) \ , \tag{4}$$

where $\boldsymbol{D}$ and $\boldsymbol{D}^{ep}$ are fourth-order tensors representing the elastic and elastoplastic modulus, respectively.

Flow surface

A phenomenological characteristic observed in elastoplastic materials is the existence of a limit within which the material behaves elastically. In isotropic materials, this domain is delimited by a hypersurface in the space of principal stresses, as follows:

$$\partial\Gamma = \{\boldsymbol{\sigma} | f(\boldsymbol{\sigma}, q) = 0\} \ , \tag{5}$$

where f is the flow function. This surface delimits the set of stresses that are elastically admissible (E.A.) and the set of stresses that are plastically admissible (P.A.) as follows:

$$\Gamma = \{\boldsymbol{\sigma} | f(\boldsymbol{\sigma}, q) < 0\} \text{ (E.A)}, \ \Gamma = \{\boldsymbol{\sigma} | f(\boldsymbol{\sigma}, q) \leq 0\} \text{ (P.A)} \ . \tag{6}$$

Fig. 1 illustrates, in a generically way, this domain.

The flow function is commonly described as a function of the invariants of the stress tensor and the forces associated with the internal variables related to the hardening and softening phenomenon, so that

$$f(\boldsymbol{\sigma}, q) = f(I_1, J_2, J_3, q) = f(\xi_H, \rho_H, \theta, q) = f(p, q^{eq}, \theta, q) = f(\boldsymbol{\sigma}_{oct}, \tau_{oct}, \theta, q) \ , \tag{7}$$

with

$$\begin{aligned}
&I_1 = \mathrm{tr}(\boldsymbol{\sigma}) = \sigma_{11} + \sigma_{22} + \sigma_{33} \\
&J_2 = \frac{1}{2}\mathrm{tr}(\boldsymbol{s}^2) = \frac{1}{6}\left[(\sigma_{11} - \sigma_{22})^2 + (\sigma_{22} - \sigma_{33})^2 + (\sigma_{33} - \sigma_{11})^2\right] + \sigma_{12}^2 + \sigma_{23}^2 + \sigma_{13}^2, \\
&J_3 = \frac{1}{3}\mathrm{tr}(\boldsymbol{s}^3) = \det(\boldsymbol{s}) = s_{11}s_{22}s_{33} - s_{11}\sigma_{23}^2 - s_{22}\sigma_{13}^2 - s_{33}\sigma_{12}^2 + 2\sigma_{12}\sigma_{23}\sigma_{13}, \\
&\xi_H = p = \sigma_{oct} = \frac{1}{3}I_1, \quad \rho_H = \sqrt{\boldsymbol{s} : \boldsymbol{s}} = \sqrt{2J_2}, \quad \theta = \frac{1}{3}\mathrm{asin}\left(\frac{-3\sqrt{3}}{2}\frac{J_3}{J_2^{3/2}}\right), \\
&-\frac{\pi}{6} \leq \theta \leq \frac{\pi}{6}, \quad q^{eq} = \sqrt{\frac{3}{2}\boldsymbol{s} : \boldsymbol{s}} = \sqrt{3J_2}, \quad \tau_{oct} = \sqrt{\frac{3}{2}J_2}, \quad \text{and} \quad \boldsymbol{s} = \boldsymbol{\sigma} - \frac{p}{3}\mathbf{1}.
\end{aligned} \tag{8}$$

In Eq. (7), I_1 is the first invariant of the stress tensor, J_2, J_3 is the second and the third invariant of the deviator tensor $\boldsymbol{s}$, (ξ_H, ρ_H, θ) are the coordinates of Haigh-Westergaard (where θ is also known as the angle of Lode), p is the hydrostatic pressure, q^{eq} is the equivalent stress of von-Mises, $(\boldsymbol{\sigma}_{oct}, \tau_{oct})$ the normal stress and the octahedral shear, respectively (Chen and Han 1988).

When the flow function does not depend of I_1, it is said that the plasticity is independent of pressure, being determined only by the state of stresses along the desviator plane (Fig. 1). Several flow functions can be found in the literature as in Chen and Han (1988), Souza Neto et al. (2008) and Zienkiewicz and Cormeau (1974). Here is used the Drucker-Prager flow surface as:

$$f(\boldsymbol{\sigma}, q) = f(I_1, J_2, \beta_i) = \beta_1 I_1 + \beta_2 \sqrt{J_2} - \beta_3, \tag{9}$$

where the β_i parameters are related to the c cohesion and the ϕ friction angle of the Mohr-Coulomb model. For the case where the surface of Drucker-Prager coincides with the surface of Mohr-Coulomb by the outer edges (DP-I) (Bernaud 1991):

$$\beta_1 = \frac{(k-1)}{3}, \quad \beta_2 = \frac{(k+2)}{\sqrt{3}}, \quad \beta_3 = 2\sqrt{k}\, c, \tag{10}$$

where $k = (1 + sin\phi)/(1 - sin\phi)$. For the case where the surface of Drucker-Prager is inscribed on the surface of Mohr-Coulomb (DP-II) (Bernaud 1991):

$$\beta_1 = \frac{(k-1)}{3}, \quad \beta_2 = \frac{(2k+1)}{\sqrt{3}}, \quad \beta_3 = 2\sqrt{k}\, c, \tag{11}$$

Plastic flow rule

The law of evolution of plastic deformation (known as plastic flow rule) is postulated as

$$\boldsymbol{\varepsilon}^p = \dot{\lambda} g^{vp} \quad \text{with} \quad \boldsymbol{g}_{\sigma} = \frac{\partial g}{\partial \boldsymbol{\sigma}}\ , \tag{12}$$

where λ is the plastic multiplier and $\boldsymbol{g}_{\sigma}$ is the tensor that gives the direction of plastic flow through the gradient of a potential function g analogous to f. Like the flow function, the plastic potential is usually described using the invariants of the stress tensor and $\boldsymbol{g}_{\sigma}$ can be determined using the chain rule. For example, if $g(I_1, \sqrt{J_2}, J3, q)$ as in Viladkar et al. (1995), we have:

$$
\begin{aligned}
&\boldsymbol{g}_{\boldsymbol{\sigma}} = C_1 \boldsymbol{g}_1 + C_2 \boldsymbol{g}_2 + C_3 \boldsymbol{g}_3, \\
&\boldsymbol{g}_1 = \frac{\partial I_1}{\partial \boldsymbol{\sigma}} = \mathbf{1}, \quad \boldsymbol{g}_2 = \frac{\partial \sqrt{J_2}}{\partial \boldsymbol{\sigma}} = \frac{1}{2\sqrt{J_2}} \boldsymbol{s}, \quad \boldsymbol{g}_3 = \frac{\partial J_3}{\partial \boldsymbol{\sigma}}, \\
&C_1 = \frac{\partial g}{\partial I_1}, \quad C_2 = \frac{\partial g}{\partial \sqrt{J_2}} - \frac{\tan(3\theta)}{\sqrt{J_2}} \frac{\partial g}{\partial \theta}, \quad C_3 = -\frac{\sqrt{3}}{2\cos(3\theta)} \frac{1}{J_2^{3/2}} \frac{\partial g}{\partial \theta}
\end{aligned}
\tag{13}
$$

As can be seen in Eq. (13), the constants C_1, C_2 and C_3 are particularities of each type of potential function. In Viladkar et al. (1995) it is possible to obtain the value of these constants for several functions, such von-Mises, Tresca, Drucker-Prager, Mohr-Coulomb, Cap Models, etc. For Drucker-Prager potential flow has $C_1 = \beta_1$, $C_2 = \beta_2$, $C_3 = 0$.

A common aspect in geomechanics is the variation of the volume of the material during the evolution of plastic deformations. This effect is commonly introduced through unassociated plasticity, adopting, instead of the friction angle a angle of dilatance $0 < \psi < \phi$ in the potencial function g.

Hardening-Softening law

The hardening-softening law characterizes the dependence of internal variables during the evolution of plastic deformations. This law is postulated as follows:

$$
\dot{q} = \dot{\lambda} h_q(\boldsymbol{\sigma}, q) = -\dot{\lambda} \frac{\partial h}{\partial q} \,, \tag{14}
$$

where $h_q = -\partial h / \partial q$ is a gradient of a potential fucntion h with respect to the associated thermodynamic forces q. As the flow function f is dependent on q, changing along the plastic deformation will change the position and/or shape of the flow surface. When the flow surface is static, that is, $\dot{q} = 0$, there is perfect plasticity, when increases, there is isotropic hardening and when it moves, there is kinematic hardening, being mixed, when composed of the last two. The associated hardening/softening law ($h = f$) and isotropic is considered. The associated thermodynamic force is given exclusively by the portion that does not depend on the hydrostatic (I_1) or deviating (J_2) part on the flow surfaces. This force is controlled by the cohesive parameter, so $q = \chi c(\bar{\varepsilon}^p) = 2\sqrt{k} c(\bar{\varepsilon}^p)$, where $\bar{\varepsilon}^p$ is the state variable. For cohesion, it is considered a linear function defined by parts, as Eq. (15), in order to represent the characteristic hadrening/softening of the rock mass.

$$c(\bar{\epsilon}^p) = \begin{cases} c_i + \dfrac{(c_p - c_i)}{\bar{\epsilon}^p_I}\bar{\epsilon}^p & \text{for zone I} \\ c_p, & \text{for zone II} \\ c_p + \dfrac{(c_r - c_p)}{\bar{\epsilon}^p_r - \bar{\epsilon}^p_{II}}(\bar{\epsilon}^p - \bar{\epsilon}^p_{II}), & \text{for zone III} \\ c_r, & \text{for zone IV} \end{cases}. \tag{15}$$

Therefore, using the chain rule in Eq. (14) we have

$$\dot{q} = -\dot{\lambda}\frac{\partial h}{\partial q} = -\dot{\lambda}\frac{\partial f}{\partial q} = \dot{\lambda}\left(-\frac{\partial f}{\partial q}\frac{\partial q}{\partial c}\frac{\partial c}{\partial \bar{\epsilon}^p}\right) = \dot{\lambda}\left(\chi\frac{\partial c}{\partial \bar{\epsilon}^p}\right), \tag{16}$$

where

$$\frac{\partial c}{\partial \bar{\epsilon}_p} = \begin{cases} \dfrac{(c_p - c_i)}{\bar{\epsilon}^p_I} & \text{for zone I} \\ 0, & \text{for zone II} \\ \dfrac{(c_r - c_p)}{\bar{\epsilon}^p_r - \bar{\epsilon}^p_{II}}, & \text{for zone III} \\ 0, & \text{for zone IV} \end{cases}. \tag{17}$$

The equivalent plastic deformation is calculated from the following expression:

$$\dot{\bar{\epsilon}}^p = C||\dot{\boldsymbol{\varepsilon}^p}||, \tag{18}$$

where

$$||\dot{\boldsymbol{\varepsilon}^p}|| = \sqrt{(\dot{\varepsilon}^p_{11})^2 + (\dot{\varepsilon}^p_{22})^2 + (\dot{\varepsilon}^p_{33})^2 + 2(\dot{\varepsilon}^p_{12})^2 + 2(\dot{\varepsilon}^p_{23})^2 + 2(\dot{\varepsilon}^p_{13})^2} \tag{19}$$

and

$$C = \frac{\beta_1 + 1/\sqrt{3}}{\sqrt{3\beta_1^2 + 1/2}}. \tag{20}$$

When $\phi = 0$ the rockmass is independent of the hydrostatic pressure $\beta = 0$ and $C = \sqrt{2/3}$.

Loading and unloading conditions

The evolution of Eq. (12) and Eq. (14) are subject to three conditions (conditions of Kuhn-Tucker), which are:

$$f \leq 0, \quad \dot{\lambda} \geq 0, \quad \dot{\lambda} f = 0. \tag{21}$$

These conditions establish that plastic flow only occurs when the state of stresses is on the flow surface and, in this case, there is no variation of the flow function in relation to the stresses, that is:

$$\dot{f} = \frac{\partial f}{\partial \boldsymbol{\sigma}} : \dot{\boldsymbol{\sigma}} + \frac{\partial f}{\partial q} \cdot \dot{q} = \boldsymbol{f_\sigma} : \dot{\sigma} + f_q \cdot \dot{q} = 0. \tag{22}$$

Eq. (22) is known as the consistency condition.

Plastic multiplier and continuous Elastoplastic Module

Introducing Eq. (22) to Eq. (28) and Eq. (14), together with Eq. (12), and isolating the plastic multiplier, we have:

$$\dot{\lambda} = \frac{\boldsymbol{f_\sigma} : \boldsymbol{D} : \dot{\boldsymbol{\varepsilon}}}{\boldsymbol{f_\sigma} : \boldsymbol{D} : \boldsymbol{g_\sigma} - f_q \cdot h_q} \tag{23}$$

that introducing in the constitutive relation Eq. (28) leads to

$$\boldsymbol{D}^{ep} = \boldsymbol{D} - \frac{(\boldsymbol{D} : \boldsymbol{g_\sigma}) \otimes (\boldsymbol{f_\sigma} : \boldsymbol{D})}{\boldsymbol{f_\sigma} : \boldsymbol{D} : \boldsymbol{g_\sigma} - f_q \cdot h_q} \tag{24}$$

where $\otimes$ is the tensorial product.

VISCOPLASTIC CONSTITUTIVE MODEL

Decomposition of the strain tensor

The viscoplastic constitutive model has a rationale similar to that of elastoplasticity, which leads to the following relationship:

$$\dot{\boldsymbol{\sigma}} = \boldsymbol{D}^{vp} : \dot{\boldsymbol{\varepsilon}} = \boldsymbol{D} : \dot{\boldsymbol{\varepsilon}}^e = \boldsymbol{D} : (\dot{\boldsymbol{\varepsilon}}^e - \dot{\boldsymbol{\varepsilon}}^{vp}) \tag{25}$$

where $\boldsymbol{D}^{vp}$ is the viscoplastic fourth order tensor.

Flow surface

Viscoplasticity does not always have an elastic domain, for example, at high temperatures certain materials can always flow under stress, that is, the flow function is zero. For these materials there are explicit functions. However, in problems involving deep tunnels, the phenomenon occurs from a certain level of stress, as described by Rousset (1988). For these cases, surfaces f^{vp} similar to those of elastoplasticity are used.

Viscoplastic flow rule and hadrening-softening law

Analogous to elastoplasticity, the viscoplastic flow rule and the hardening-softening law are postulated as follows:

$$\begin{aligned} \boldsymbol{\varepsilon}^{vp} &= \dot{\lambda}^{vp} \boldsymbol{g}_{\boldsymbol{\sigma}}{}^{vp} \quad \text{with} \quad \boldsymbol{g}_{\boldsymbol{\sigma}} = \frac{\partial g^{vp}}{\partial \boldsymbol{\sigma}}, \\ \dot{q}^{vp} &= \dot{\lambda}^{vp} h_q(\boldsymbol{\sigma}, q^{vp}) = -\dot{\lambda}^{vp} \frac{\partial h^{vp}}{\partial q^{vp}} \quad \text{and} \quad \bar{\varepsilon}^{vp} = \int_0^t \dot{\lambda}^{vp} dt \,. \end{aligned} \tag{26}$$

However, in this work , the viscoplasticity is perfect, that is, $\dot{q}^{vp} = 0$.

Viscoplastic multiplier

Unlike elastoplasticity, viscoplastic deformation occur even when $f^{vp} > 0$, and therefore, the consistency condition is not imposed. Thus, the rate of the viscoplastic multiplier λ^{vp} cannot be obtained from a condition like $\dot{f}^{vp} = 0$. Therefore, there are models that provide an explicit expression for and in this work Perzyna model (Perzyna 1966) will be adopted, as described in Zienkiewicz and Cormeau (1974):

$$\dot{\lambda}^{vp} = \frac{\Phi(\boldsymbol{\sigma}, q^{vp})}{\eta} \quad \text{and} \quad \Phi = \left\langle \frac{f(\boldsymbol{\sigma}, q^{vp})}{f_0} \right\rangle^n \tag{27}$$

where Φ is the overstress function, η is the dynamic viscosity constant, n is the dimensionless parameter that gives the form of the power law , f_0 a parameter conveniently adopted and $\langle * \rangle$ is the McCauley function which is null when $* < 0$, that is, viscoplastic flow will only occur when the criterion is positive.

ELASTOPLASTIC-VISCOPLASTIC CONSTITUTIVE MODEL

The proposed elastoplastic-viscoplastic model is constructed by the serial association of the constitutive models described above, and, therefore, we have:

$$\dot{\boldsymbol{\sigma}} = \boldsymbol{D}^{vp} : \dot{\boldsymbol{\varepsilon}} = \boldsymbol{D} : \dot{\boldsymbol{\varepsilon}}^{e} = \boldsymbol{D} : \left(\dot{\boldsymbol{\varepsilon}}^{e} - \dot{\boldsymbol{\varepsilon}}^{vp}\right) . \tag{28}$$

This association can be seen in the one-dimensional representation of Fig. 2. An important observation is that the flow surfaces and the internal variables that define the elastoplastic and viscoplastic portion of this model can be different from each other, including the association of their respective potential functions with their flow surfaces. Generally, viscoplasticity parameters are chosen so that its viscoplastic surface is inside the elastoplastic-viscoplastic surface, thus having the domains represented in Fig. 3.

SOLUTION OF NONLINEAR CONSTITUTIVE PROBLEMS IN FINITE ELEMENTS

Though the weak form of the field equations that govern the problem and the spatial discretization of the domain in finite elements, for quasi-static problems, isothermal in small transformations, we have the following set of nodal equations to be solved:

$$\left(\boldsymbol{K}\,\boldsymbol{u} + \boldsymbol{F}_{\varepsilon_0} + \boldsymbol{F}_{\sigma_0}\right) - \left(\boldsymbol{F}_V + \boldsymbol{F}_S + \boldsymbol{F}_N\right) = \boldsymbol{F}_{int} - \boldsymbol{F}_{ext} = f(\boldsymbol{u}) = \underline{0} \tag{29}$$

where $\boldsymbol{K}$ is the global stiffness matrix resulting from the assembly of the stiffness matrices of each element $\boldsymbol{K}_e$, $\boldsymbol{u}$ is the incognito vector of global nodal displacements resulting from the assembly of nodal displacements $\boldsymbol{u}_e$ of each element, $(\boldsymbol{F}_V,\ \boldsymbol{F}_S,\ \boldsymbol{F}_N)$ are the global forces resulting from volume, surface and nodal from the assembly of respective forces of each element and $(\boldsymbol{F}_{\sigma_0},\ \boldsymbol{F}_{\varepsilon_0})$ are the global forces resulting from intial stresses σ_0 and initial strains ε_0 of each element.

When there is non-linearity involving the constitutive laws of the materials, the coefficient matrix $\boldsymbol{K}$ becomes dependent on the unknown nodal displacements $\boldsymbol{u}$, making the system non-linear. The Newton-Raphson method is the iterative process commonly used to solve this system. Therefore, approximating the system by a Taylor series truncated in the first order, we have the following iterative expression to approximate $\boldsymbol{u}$:

$$\boldsymbol{u}_{i+1} = \boldsymbol{u}_i - \boldsymbol{K}(\boldsymbol{u}_i)^{-1}\left(\boldsymbol{F}_{int}(\boldsymbol{u}_i) - \boldsymbol{F}_{ext}\right) = \boldsymbol{u}_i - \boldsymbol{K}_i^{-1}\left(\boldsymbol{F}_{int_i} - \boldsymbol{F}_{ext}\right) = \boldsymbol{u}_i + \boldsymbol{K}_i^{-1}\boldsymbol{R}_i = \boldsymbol{u}_i + \Delta\boldsymbol{u}_i \quad (30)$$

where $\Delta\boldsymbol{u}_i$ is the increment of nodal displacemetns of current iteration of the current iteration i, $\boldsymbol{F}_{int}$ are the internal forces of current iteration, $\boldsymbol{R}_i$ is the unbalanced load vector (also called residual) for the current iteration, $\boldsymbol{K}_i$ is the tangent global matrix, $\boldsymbol{u}_i$ are the node displacements in the current iteration and $\boldsymbol{u}_{i+1}$ are the updated nodal displacements.

In order to incorporate the dependence of the load history, Eq. (30) is discretized into $1 \leq n \leq n_s$ substeps in which the external load and or time are linearly incremented, and therefore:

$$\begin{aligned}
&\Delta\boldsymbol{u}_{n,i} = \boldsymbol{K}_{n,i}^{-1}\left(\boldsymbol{F}_{ext_n} - \boldsymbol{F}_{int_{n,i}}\right) = \boldsymbol{K}_{n,i}^{-1}\boldsymbol{R}_{n,i}, \quad \boldsymbol{u}_{n,i+1} = \boldsymbol{u}_{n,i} + \Delta\boldsymbol{u}_{n,i},\\
&\boldsymbol{F}_{ext_n} = \boldsymbol{F}_{ext_{n-1}} + \Delta\boldsymbol{F}_p, \quad t_n = t_{n-1} + \Delta t_p, \quad \boldsymbol{F}_{int_{n,i}} = \left(\int_\Omega \boldsymbol{B}^T\boldsymbol{\sigma}\, d\Omega\right)_{n,i},\\
&n_s = \frac{t_p}{\Delta t_p}, \quad \Delta\boldsymbol{F}_p = \frac{\boldsymbol{F}_{ext_p}}{n_s},
\end{aligned} \quad (31)$$

where $\boldsymbol{B} = \nabla^s\boldsymbol{N}$, $\boldsymbol{N}$ are the array containing the finite element shape functions and ∇^s is symmetric gradient operator. In the computational implementation it is common to use the matrix form given by Voigt's rules (Belytschko et al. 2000) instead of the tensor representation. In this paper, the Voigt's notation will be used, but with the same symbology as tensor notation.

In Eq. (31) $\boldsymbol{F}_{ext_n}$ and t_n are the external forces and the time at the end of the step, respectively. At the beginning of the iterative process $u_{0,0}$, $\boldsymbol{F}_{int_{0,0}}$, $\boldsymbol{F}_{ext_0}$ and t_0 are null. For the next substeps, the values of $u_{n,0}$ e $\boldsymbol{F}_{int_{n,0}}$ correspond to the values of the previous solution $n-1$.

ALGORITHM FOR UPDATING THE STRESS AND INTERNAL VARIABLES

The algorithms for updating stress and internal variables propose to solve the system of differential equations involving the constitutive relations through some integration scheme (generally Runge-Kutta). The algorithm occurs for each Gauss point of each element during the equilibrium iterations and, given a known set of $\left\{\boldsymbol{\varepsilon}_n, \boldsymbol{\varepsilon}_n^p, \boldsymbol{\sigma}_n, q_n\right\}$ in the substep n and the increment of total strain $\Delta\boldsymbol{\varepsilon}$ we try to obtain the values of the next substep $\left\{\boldsymbol{\varepsilon}_{n+1}, \boldsymbol{\varepsilon}_{n+1}^p, \boldsymbol{\sigma}_{n+1}, q_{n+1}\right\}$ where $\boldsymbol{\varepsilon}_{n+1}^{in}$ is the inelastic strain (plastic or viscoplastic).

Integration of elastoplastic constitutive equations

Using the first order Runge-Kutta method we have the following scheme of integration of the constitutive equations:

$$\begin{cases} \boldsymbol{\varepsilon}_{n+1} = \boldsymbol{\varepsilon}_n + \Delta\boldsymbol{\varepsilon} \\ \boldsymbol{\varepsilon}^p_{n+1} = \boldsymbol{\varepsilon}^p_n + \left[(1-\Theta)\Delta\lambda_n \boldsymbol{g}_{\boldsymbol{\sigma}n} + \Theta\Delta\lambda_{n+1}\boldsymbol{g}_{\boldsymbol{\sigma}n+1}\right] \\ q_{n+1} = q_n + \left[(1-\Theta)\Delta\lambda_n h_{q_n} + \Theta\Delta\lambda_{n+1} h_{q_{n+1}}\right] \\ \boldsymbol{\sigma}_{n+1} = \boldsymbol{D}\,\boldsymbol{\varepsilon}^e_{n+1} = \boldsymbol{D}(\boldsymbol{\varepsilon}_{n+1} - \boldsymbol{\varepsilon}^p_{n+1}) \\ f_{n+1} = f(\boldsymbol{\sigma}_{n+1}, q_{n+1}) = 0 \end{cases} \tag{32}$$

where $\Delta\lambda = \dot{\lambda}\Delta t$ and $0 \leq \Theta \leq 1$ provides the generalized trapezoidal rule for plastic flow and the evolution of internal variables. When $\Theta = 0$ we obtain the form fully explicit and $\Theta = 1$ the fully implicit. Semi-implicit algorithms adopt $0 \leq \Theta < 1$ or a combination of implicit and explicit of the $\Delta\lambda$, $\boldsymbol{g}_{\boldsymbol{\sigma}}$ e h_q.

The completely explicit schemes, for example, adopted in Nayak and Zienkiewicz (1972), Zienkiewicz et al. (1969) and Owen and Hinton (1980), were widely used until Simo and Taylor (1985) proposed an implicit two-step predictor-corrector method. The completely explicit schemes did not satisfy the consistency condition $f_{n+1} = f(\boldsymbol{\sigma}_{n+1}, q_{n+1})$ at the end of the substep, since the plastic multiplier and the flow vectors were calculated with the stress of the previous substep n. Currently, completely implicit or semi-implicit algorithms that satisfy $f_{n+1} = 0$ are used and some semi-implicit ones avoid the need to calculate the second order gradients of flow vectors $\boldsymbol{g}_{\boldsymbol{\sigma}}$ and h_q, but need more equilibrium iterations in relation to the fully implicit scheme. Several integration schemes for elastoplasticity can be found in Souza Neto et al. (2008), Belytschko et al. (2000) and Simo and Hughes (1998). In this work, a semi-implicit two-step integration scheme, present in Belytschko et al. (2000), in which the plastic multiplier is integrated through an implicit scheme and the flow vectors are explicitly integrated.

Two-step integration schemes have two steps: first, the elastic predictor is calculated and, if necessary, the plastic corretor. Defining $\Delta\boldsymbol{\varepsilon}^p_{n+1} \equiv \boldsymbol{\varepsilon}_{n+1} - \boldsymbol{\varepsilon}_n$, the elastic predictor can be explained from Eq. $(32)_4$ as:

$$\boldsymbol{\sigma}_{n+1} = \boldsymbol{D}(\boldsymbol{\varepsilon}_{n+1} - \boldsymbol{\varepsilon}^p_{n+1}) = \boldsymbol{D}(\boldsymbol{\varepsilon}_n + \Delta\boldsymbol{\varepsilon} - \boldsymbol{\varepsilon}^p_n - \Delta\boldsymbol{\varepsilon}^p_{n+1}) = \boldsymbol{\sigma}^{trial}_{n+1} + \Delta\boldsymbol{\sigma}_{n+1} \tag{33}$$

where $\boldsymbol{\sigma}^{trial}_{n+1} = \boldsymbol{D}(\boldsymbol{\varepsilon}_n + \Delta\boldsymbol{\varepsilon} - \boldsymbol{\varepsilon}^p_n)$ is the elastic predictor (also known as trial stress). Thus, in the first step, the trial stress is calculated and the flow function f . If $f < 0$ the stress state is in the elastic domain and there is no need to apply the plastic corrector. However, if $f > 0$ the stress state is outside the plastically admissible domain, it is necessary to apply the plastic corrector step.

The plastic corrector is nothing more than the system solution procedure Eq. $(32)_{2,3,5}$ which will determine the increments $\Delta\boldsymbol{\sigma}_{n+1}$ and Δq_{n+1}. When it is not possible to obtain an analytical solution for this system, the commonly used solution procedure is the Newton-Raphson one, which iterates k times through the space of the stresses and internal variables until the stress state returns on the flow surface. This is why these schemes are also known as return mapping algorithms. Fig. 4 geometrically illustrates this solution.

Therefore, to solve by Newton-Raphson the system that gives the beginning to the plastic corrector writes in the in the following residual (omitting the index $n + 1$):

$$\begin{cases} \boldsymbol{a} = -\boldsymbol{\varepsilon}^p + \boldsymbol{\varepsilon}^p_n + \Delta\lambda \boldsymbol{g}_{\sigma n} = \boldsymbol{0} \\ \boldsymbol{b} = -q + q_n + \Delta\lambda h_{q_n} = \boldsymbol{0} \\ f = f(\boldsymbol{\sigma}, q) = 0 \end{cases} . \tag{34}$$

Linearizing the Eq. (34) in relation to $\Delta\lambda$, knowing that $\Delta\boldsymbol{\varepsilon}^p = -\boldsymbol{D}^{-1}\Delta\boldsymbol{\sigma}$ give:

$$\begin{cases} \boldsymbol{a}_k + \boldsymbol{D}^{-1}\Delta\boldsymbol{\sigma}_k + \delta\lambda_k \boldsymbol{g}_{\sigma n} = \boldsymbol{0} \\ \boldsymbol{b}_k - \Delta q_k + \delta\lambda_k h_{q_n} = \boldsymbol{0} \\ f_k + \boldsymbol{f}_{\sigma k}^T \Delta\boldsymbol{\sigma}_k + f_{q k}^T \Delta q_k = 0 \end{cases} . \tag{35}$$

Eq. (35) comprise a system of three equations with three unkowns: $\Delta\boldsymbol{\sigma}_k$, Δq_k and $\delta\lambda_k$ and as the flow vectors $\boldsymbol{g}_{\boldsymbol{\sigma}}$ and h_q are calculated in the initial step n, their gradients did not appear in the formulations. Reorganizing this system we obtain the following solution for the plastic corrector:

$$\begin{Bmatrix} \Delta\boldsymbol{\sigma}_k \\ \Delta q_k \end{Bmatrix} = -\delta\lambda_k \, [\boldsymbol{A}] \begin{Bmatrix} \boldsymbol{g}_{\sigma n} \\ h_{q_n} \end{Bmatrix} \tag{36}$$

$$[\boldsymbol{A}] = \begin{bmatrix} \boldsymbol{D} & \boldsymbol{0} \\ \boldsymbol{0} & -\boldsymbol{1} \end{bmatrix}. \tag{37}$$

$$\delta\lambda_k = \frac{f_k}{\begin{bmatrix} \boldsymbol{f}_{\sigma}{}_k^T & f_{q}{}_k^T \end{bmatrix} [\boldsymbol{A}] \begin{Bmatrix} \boldsymbol{g}_{\sigma n} \\ h_{q_n} \end{Bmatrix}} \tag{38}$$

Due to this explicit treatment of the flow vectors in Eq. (37), $[\boldsymbol{A}]$ presents a closed expression involving only the elastic modulus. In addition, as the system Eq. (35) is composed of linear functions in relation to $\Delta\lambda$ the residuals $\boldsymbol{a}_k$ and $\boldsymbol{b}_k$ will automatically be null, dispensing its verification in the convergence criterion, as pointed by Belytschko et al. (2000).

After updating the stresses and internal variables, it is possible to update the constitutive module. It is possible to use the tangent modulus consistent with the linearization made during the algorithm for integrating the constitutive laws (that is why this modulus is also known as the algorithmic modulus). Its use increase the convergence rate of equilibrium iterations. Its general expression is defined by:

$$\boldsymbol{D}^{alg} = \left(\frac{d\boldsymbol{\sigma}}{d\boldsymbol{\varepsilon}}\right)_{n+1}. \tag{39}$$

To derive the expression from $\boldsymbol{D}^{alg}$ resolves Eq. (32) to $d\boldsymbol{\sigma}/d\boldsymbol{\varepsilon}$ (Belytschko et al. 2000). With that, we have, for elastoplasticity, the following relationship (omitting the $n+1$ index):

$$\boldsymbol{D}^{alg} = \boldsymbol{D} - \frac{\boldsymbol{D}\,\boldsymbol{g}_{\sigma n}\,\boldsymbol{f}_{\sigma}{}^T\boldsymbol{D}}{\boldsymbol{f}_{\sigma}{}^T\boldsymbol{D}\,\boldsymbol{g}_{\sigma i} - f_q h_{q_n}} \tag{40}$$

The flowchart can be seen in Fig. 5.

Integration of viscoplastic constitutive equations

Different integration algorithms can be found in the literature, such as in Cormeau (1975), Hughes and Taylor (1978), Marques and Owen (1983), Pierce et al. (1984), Bernaud (1991) and some of the most used in Belytschko et al. (2000), Souza Neto et al. (2008), Huang and Griffiths (2009) and Smith et al. (2014). For the present work, a scheme introduced by Pierce et al. (1984), known as the Rate Tangent Modulus Method, which comprises an explicit Euler scheme for all variables, except for $\Delta\lambda^{vp}$ that is integrated according to the generalized trapezoidal rule. So, we have the following scheme:

$$\begin{cases} \boldsymbol{\varepsilon}_{n+1} = \boldsymbol{\varepsilon}_n + \Delta\boldsymbol{\varepsilon} \\ \boldsymbol{\varepsilon}^{vp}_{n+1} = \boldsymbol{\varepsilon}^{vp}_n + \Delta\lambda^{vp}\boldsymbol{g}_{\sigma}{}^{vp}_n \\ q^{vp}_{n+1} = q^{vp}_n + \Delta\lambda^{vp} h_{q}{}^{vp}_n \\ \boldsymbol{\sigma}_{n+1} = \boldsymbol{D}\ \boldsymbol{\varepsilon}^{e}_{n+1} = \boldsymbol{D}(\boldsymbol{\varepsilon}_{n+1} - \boldsymbol{\varepsilon}^{vp}_{n+1}) \\ \Delta\lambda = \dfrac{\Delta t}{\eta}[(1-\Theta)\Phi_n + \Theta\Phi_{n+1}] \end{cases}. \tag{41}$$

Linearizing the overstress of Eq. (27) we have:

$$\Phi_{n+1} = \Phi_n + \boldsymbol{\Phi}_{\sigma}{}^{T}_{n}\Delta\boldsymbol{\sigma} + \boldsymbol{\Phi}_{\boldsymbol{q}}{}^{T}_{n}\Delta q^{vp} \tag{42}$$

where $\boldsymbol{\Phi}_{\sigma} = \partial\Phi/\partial\boldsymbol{\sigma}$ e $\boldsymbol{\Phi}_{\boldsymbol{q}} = \partial\Phi/\partial q$. Replacing Eq. (42) in the Eq. $(41)_5$ we obtain:

$$\Delta\lambda = \frac{\Delta t}{\eta}\Phi_n + \frac{\theta\Delta t}{\eta}(\boldsymbol{\Phi}_{\sigma}{}^{T}_{n}\Delta\boldsymbol{\sigma} + \boldsymbol{\Phi}_{\boldsymbol{q}}{}^{T}_{n}\Delta q). \tag{43}$$

And introducing Eq. $(41)_2$ into Eq. $(41)_4$ and rewriting Eq. $(41)_3$ we obtain:

$$\begin{Bmatrix} \Delta\boldsymbol{\sigma} \\ \Delta q^{vp} \end{Bmatrix} = \begin{Bmatrix} \boldsymbol{D}(\Delta\boldsymbol{\varepsilon} - \Delta\lambda^{vp}\boldsymbol{g}_{\sigma n}) \\ \Delta\lambda^{vp} h_{q}{}^{vp}_{n} \end{Bmatrix}. \tag{44}$$

Finally, replacing (44) in (43) we can isolate $\Delta\lambda^{vp}$:

$$\Delta\lambda^{vp} = \frac{\Phi_n + \Theta\boldsymbol{\Phi}_{\sigma n}^{\ T}\boldsymbol{D}\Delta\boldsymbol{\varepsilon}}{\dfrac{\eta}{\Delta t} + \Theta(\boldsymbol{\Phi}_{\sigma n}^{\ T}\boldsymbol{D}\ \boldsymbol{g}_{\sigma n}^{\ vp} - \boldsymbol{\Phi}_{\boldsymbol{q}n}^{\ T} h_{q_n}^{\ vp})}. \tag{45}$$

When $0 < \Theta < 1$ we have a semi-implicit algorithm and when $\Theta = 0$ we have a totally explicit algorithm, with $\Delta\lambda^{vp} = \Delta t \dfrac{\Phi_n}{eta}$. As can be seen from this deduction, unlike the integration of the constitutive relationship in elastoplasticity, there is no need to solve the system iteratively. And, in addition, all variables are taken from the previous n substep. This fact, as will be seen in the next section, will facilitate the coupling between the viscoplasticity and elastoplasticity algorithm. Furthermore, for viscoplasticity, hardening-softening laws are not used, simplifying the expression (44) to:

$$\Delta\lambda^{vp} = \frac{\Phi_n + \Theta\boldsymbol{\Phi}_{\sigma n}^{\ T}\boldsymbol{D}\Delta\boldsymbol{\varepsilon}_n}{\dfrac{\eta}{\Delta t} + \Theta\boldsymbol{\Phi}_{\sigma n}^{\ T}\boldsymbol{D}\boldsymbol{g}_{\sigma n}}. \tag{46}$$

Substituting (46) into $(44)_1$ schema gives a closed expression for the stress update:

$$\Delta\boldsymbol{\sigma} = \boldsymbol{D}^{alg}\Delta\boldsymbol{\varepsilon} - \boldsymbol{p} \tag{47}$$

with

$$\boldsymbol{D}^{alg} = \boldsymbol{D} - \frac{\Theta\boldsymbol{D}\ \boldsymbol{g}_{\sigma n}\ \boldsymbol{\Phi}_{\sigma n}^{\ T}\boldsymbol{D}}{\eta/\Delta t + \Theta\boldsymbol{\Phi}_{\sigma n}^{\ T}\boldsymbol{D}\ \boldsymbol{g}_{\sigma n}}, \quad \boldsymbol{p} = \frac{\Phi_n\boldsymbol{D}\ \boldsymbol{g}_{\sigma n}}{\eta/\Delta t + \Theta\boldsymbol{\Phi}_{\sigma n}^{\ T}\boldsymbol{D}\ \boldsymbol{g}_{\sigma n}} \tag{48}$$

where $\boldsymbol{D}^{alg}$ is the algorithmic constitutive modulus and $\boldsymbol{p}$ a pseudo-stress that does not depend on the increment of total strain.

The integration scheme represented by $(41)_5$ is unconditionally stable for a value of $\Theta \geq 1/2$. However, this does not guarantee the accuracy of the solution. Thus, as for values $\Theta < 1/2$, a limit value must be used for the time increment $\Delta t \leq \Delta t_{\mathrm{lim}}$. This limit can generally be achieved by reducing the time increment until the solution does not change. Strictly it depends on the material parameters, the integration scheme, the flow surface and the flow rule and there are some analytical solutions for classical surfaces. To avoid this precision problem, in this work, the limits of Drucker-Prager surface is (Cormeau 1975):

$$\Delta t_{\lim} \leq \begin{cases} \dfrac{4}{3}\dfrac{\eta}{\Phi}\dfrac{(1+\nu)}{E}\sqrt{3J_2} \\ \dfrac{\eta f_0}{\Phi'}\dfrac{(1+\nu)(1-2\nu)}{E}\dfrac{(3-\sin\phi)^2}{\frac{3}{4}(1-2\nu)(3-\sin\phi)^2+6(1+\nu)\sin\phi^2} \end{cases} \tag{49}$$

where $\phi' = \dfrac{d\phi}{d(f/f0)} = n(f/f0)^{n-1}$. When $\phi = 0$ we have the specific case for the von-Mises surface. This limit is deduced considering the associated viscoplasticity and a fully explicit integration scheme. The flowchart for the viscoplastic equations integration algorithm can be seen in Fig. 6.

Integration of elastoplastic-viscoplastic constitutive equations

As viscoplasticity is integrated through a semi-implicit rule in which all variables are calculated in substep n, that is, with the known stress, the viscoplastic strain increment can be directly discounted from the total strain increment in the elastic prediction step of the elastoplasticity algorithm. The algorithm for integrating the elastoplastic-viscoplastic constitutive equations can be seen in the flowchart of Fig. 7.

VALIDATION OF THE MODEL

As validation, a comparison will be made with the analytical and numerical solution deduced by (Piepi 1995) for a perfect elastoplastic-viscoplastic model with Tresca's criterion applied to deep clay rockmass. This analytical solution was chosen because it uses the same association principle as in Fig. 2 and will be compared with the numerical solution in axisymmetry. Furthermore, it is considered the same surface for plasticity and viscoplasticity, and their flow vectors are fully associated $f^p = g^p = f^{vp} = g^{vp}$.

The algorithm was implemented in ANSYS software through the UPF (User Programming Features). The mesh (Fig. 8) comprises 1222 linear elements of four nodes, two degrees of freedom per node and four integration points. The domain was divided into four areas to control spatial discretization. The system size, after applying the boundary conditions is of 7626 equations.

The excavation method consisted of the technique of deactivating the elements to be excavated by multiplying the modulus of elasticity by 10^{-16} (eliminating its contribution to the stiffness matrix) and making the stresses to zero in the Gauss points during the integration of internal forces. The geometric parameters are in Tab. 1.

The following constitutive parameters are used: $E = 1500\text{MPa}$ and 2000MPa, $\nu = 0.498$, $c^i = c^p = c^r = 4\sqrt{3}/2\text{MPa}$, $c^{vp} = 3\sqrt{3}/2\text{MPa}$, $\eta = 4 \cdot 10^4\text{day}$, $n = 1$, $f_0 = 1\text{MPa}$ and $p_v = p_h = 9$ MPa. The viscous phenomenon evolves over time between excavation steps. This time is calculated as the ration between the step size of the excavation L_p and the excavation speed $V_p = 10m/day$. After the last excavation the model continues incrementing the time until the deformation increment is in the order of 10^{-8}. In the latter, it can be noted that the elastoplastic model has greater cohesion than the viscoplastic model. This causes viscoplastic deformations to start even before the solid plasticize. The long-term convergence profile, that is, after the time-deferred effects cease, can be seen in Fig. 9 and Fig. 10. There is an excellent agreement between the proposed numerical solution with the analytical and numerical solution given by Piepi (1995).

PARAMETERS FOR ANALYZES

RESULTS AND DISCUSSION

CONCLUSIONS

DATA AVAILABILITY STATEMENT

Some or all data, models, or code that support the findings of this study are available from the corresponding author upon reasonable request. (ANSYS APDL script for FEM model and USERMAT suboroutine in FORTRAN90 for constitutive concrete model)

REFERENCES

Barla, G., Bonini, M., and Debernardi, D. (2008). “Time dependent deformations in squeezing tunnels.” *The 12th International Conference of International Association for Computer Methods and Advances in Geomechanics (IACMAG)*, 1–6.

Belytschko, T., Liu, W. K., and Moran, B. (2000). *Nonlinear Finite Elements for Continua and Structures*. Jhon Wiley and Sons.

Bernaud, D. (1991). “Tunnels profonds dans les milieux viscoplastiques: approches expérimentale et numérique.” Ph.D. thesis, Ecole Nationale des Ponts et Chaussées, Paris, French.

Chen, W. F. and Han, D. (1988). *Plasticity for structural engineers*. Springer-Verlag.

Cormeau, I. C. (1975). “Numerical stability in quasi-static elasto/visco-plasticity.” *International Journal for Numerical Methods in Engineering*, 9(1), 109–127.

Debernardi, D. and Barla, G. (2009). “New viscoplastic model for design analysis of tunnels in squeezing conditions.” *Rock Mechanics and Rock Engineering*, 42(2), 259–288.

Huang, J. and Griffiths, D. V. (2009). “Return mapping algorithms and stress predictors for failure analysis in geomechanics.” *Journal of engineering mechanics*, 135(4), 276–284.

Hughes, T. J. R. and Taylor, R. L. (1978). “Unconditionally stable algorithms for quasi-static elasto/viscoplastic finite element analysis.” *Computers and Structures*, 8(2), 169–173.

Kleine, A. (2007). “Modélisation numérique du comportement des ouvrages souterrains par une approche viscoplastique.” Ph.D. thesis, Institut National Polytechnique de Lorraine, Lorraine.

Manh, H. T., Sulem, J., Subrin, D., and Billaux, D. (2015). “Anisotropic time-dependent modeling of tunnel excavation in squeezing ground.” *Rock Mechanics and Rock Engineering*, 48(6), 2301–2317.

Marques, J. M. M. C. and Owen, D. R. J. (1983). “Strain hardening representation for implicit quasistatic elasto-viscoplastic algorithms.” *Computers and Structures*, 17(2), 301–304.

Nayak, G. C. and Zienkiewicz, O. C. (1972). “Elastic-plastic stress analysis: a generalization for various constitutive relations including strain softening.” *International Journal for Numerical Methods in Engineering*, 5(1), 113–135.

Owen, J. and Hinton, E. (1980). *Finite Elements in Plasticiy – Theory and Pratice*. Pinebridge Press.

Perzyna, P. (1966). “Fundamental problems in viscoplasticity.” *Advances in applied mechanics*, Vol. 9, Elsevier, 243–377.

Piepi, G. T. (1995). “Comportement viscoplastique avec rupture des argiles raides: applications aux ouvrages souterrains.” Ph.D. thesis, Ecole Nationale des Ponts et Chaussées, Paris, French.

Pierce, D., Shih, C. F., and Needleman, A. (1984). “A tangent modulus method for rate dependent solids.” *Computers and Structures*, 18(15), 875–887.

Purwodihardjo, A. and Cambou, B. (2003). “Effect of strain-softening on settlement due to tunnelling in soft soil.” *New Paradigms in Subsurface Prediction*, M. S. Rosenbaum and A. K. Turner, eds., Springer Berlin Heidelberg, 99 edition, 173–188.

Ramoni, M. and Anagnostou, G. (2010). “Thrust force requirements for tbms in squeezing ground.” *Tunnelling and Underground Space Technology*, 25(4), 433–455.

Rousset, G. (1988). “Comportement mecanique des argiles profondes: application au stockage de déchets radioactifts.” Ph.D. thesis, Ecole Nationale des Ponts et Chaussées, Paris, French.

Shafiqu, Q. S. M., Taha, M. R., and Chik, Z. H. (2008). “Finite element analysis of tunnels using the elastoplastic-viscoplastic bounding surface model.” *Journal of Engineering and Applied Sciences*, 3(3), 36–42.

Simo, J. C. and Hughes, T. J. R. (1998). *Computacional Inelasticity*. Springer-Verlag.

Simo, J. C. and Taylor, R. L. (1985). “Consistent tangente operators for rate-independent elastoplasticity.” *Comput. Methods Appl. Mech. Eng*, 49(2), 221–245.

Smith, I. M., Griffiths, D. V., and Margetts, L. (2014). *Programming the Finite Element Method*. Wiley and Sons, 5 edition.

Souley, M., Armand, G., Su, K., and Ghoreychi, M. (2011). “Modeling the viscoplastic and damage behavior in deep argillaceous rocks.” *Physics and Chemistry of the Earth, Parts A/B/C*, 36(17).

Souza Neto, E. A., Peric, D., and Owen, D. R. J. (2008). *Computational Methods for plasticity: theory and applications*. John Wiley and Sons.

Viladkar, M. N., Noorzaei, J., and Godbole, P. N. (1995). “Convenient forms of yield criteria in elasto-plastic analysis of geological materials.” *Computers and Structures*, 54(2), 327–337.

Zienkiewicz, O. C. and Cormeau, I. C. (1974). “Visco-plasticity and creep in elastic solids: a unified numerical solution approach.” *International Journal for Numerical Methods in Engineering*, 8(4), 821–845.

Zienkiewicz, O. C., Valliapan, S., and King, I. P. (1969). “Elasto-plastic solutions of engineering problems – the initial stress finite element approach.” *International Journal for Numerical Methods in Engineering*, 1(1), 75–100.

List of Tables

TABLE 1. Geometric parameters of the mesh

PARAMETERS	SYMBOL	UNIT	VALUES
		GEOMETRIC DOMAIN	
Radius of interface between tunnel and rockmass	R_i	m	1
Lining thickness	e_{rev}	m	0,1
Radius of the region near the tunnel R_1	R_1	m	$10R_i$
Total domain lenght	L_x	m	$20R_i$
Length beyond R_1	L_{x_1}	m	$L_x - R_1$
		ESCAVATION AND PLACEMENT OF LINING	
Number of excavation steps	n_p	un	38
Numeber of steps in first excavation	n_{p_i}	un	3
Length of the excavated part	Ly_1	m	$n_p L_p$
Length of unexcavated part	Ly_2	m	$25L_p$
Longitudinal length of domain	L_y	m	$L_{y_1} + L_{y_2}$
Excavation step size	L_p	m	$1/3R_i$
Unsupported dimension	d_0	m	$0,\ 2L_p,\ 4L_p$
Lining face coordinate	y_r	m	$(i_p - 1)L_p + n_{p_i}L_p - (L_p + d_0)$
Excavation face coordinate	y_f	m	$(i_p - 1)L_p + n_{p_i}L_p$
		DISCRETIZATION	
Elements along R_i	nR_i	un	5
Elements in lining thickness	n_{rev}	un	2
Elements along R_1	nR_1	un	15
First and last element ration of R_1	mR_1	adm	15
Elements along L_{x_1}	nL_{x_1}	un	5
First and last element ration of L_{x_1}	mL_{x_1}	adm	5
Element size in excavated part	L_{p_e}	m	L_p
NNumber of elements along L_{y_2}	nL_{y_2}	un	8
First and last element ratio of L_{y_2}	mL_{y_2}	adm	5

List of Figures

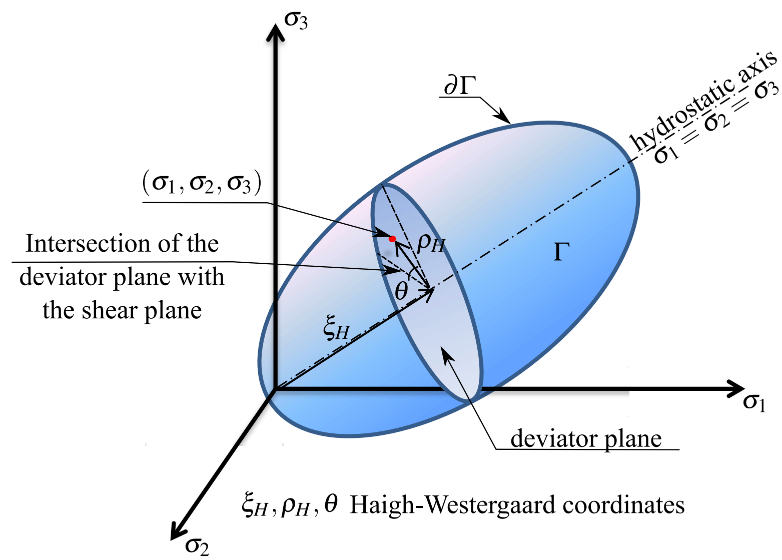

Fig. 1. Domain plasticly admissible Γ in the principal stress space.

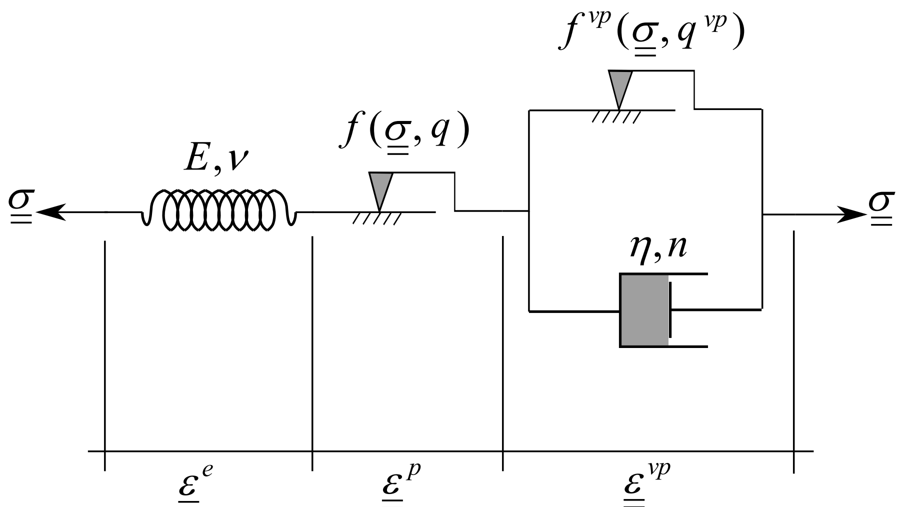

Fig. 2. Rheological representation of the elastoplastic-viscoplastic model.

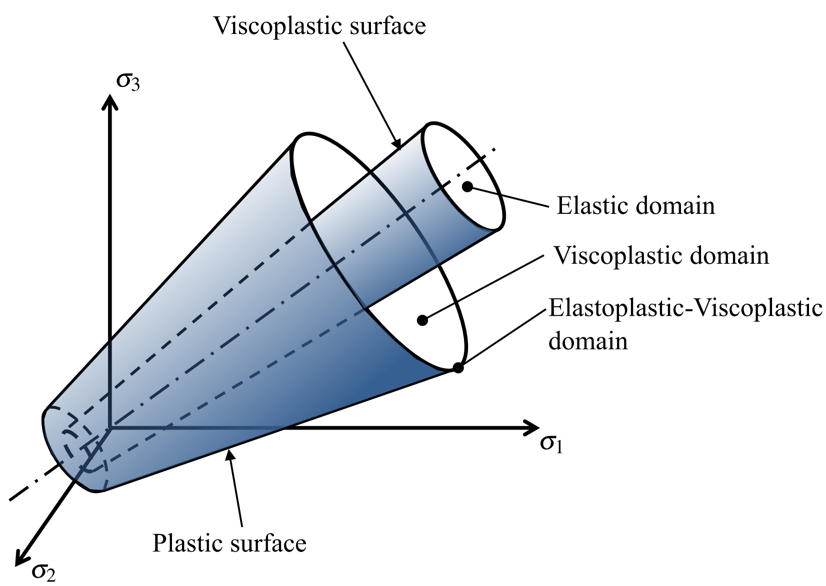

Fig. 3. Domains and surfaces of the elastoplastic-viscoplastic model.

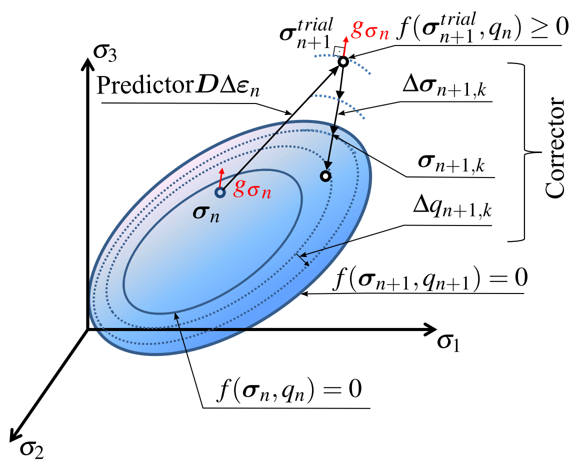

Fig. 4. Illustration of the mapped return semi-implicit with k Newton-Raphson local iterations

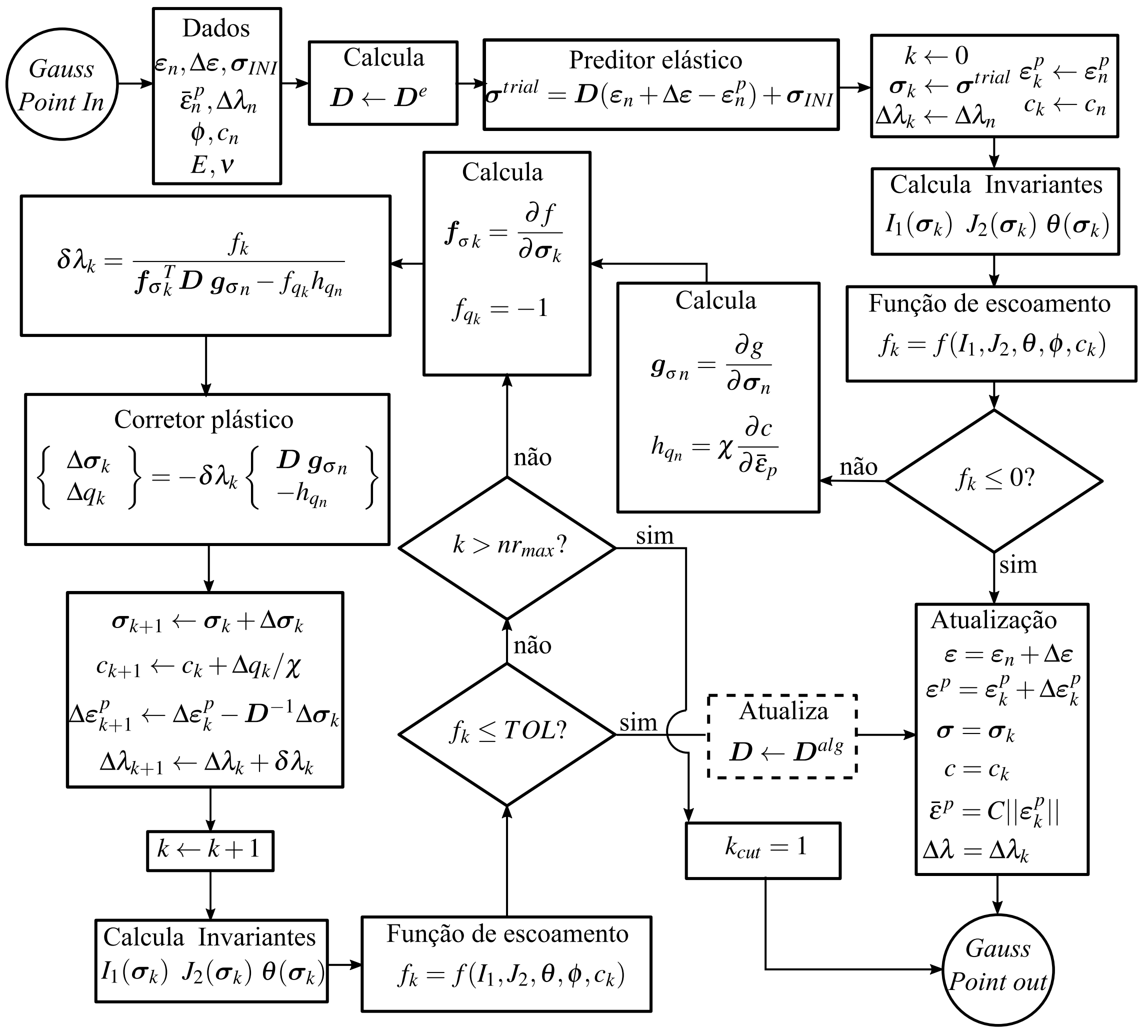

Fig. 5. Integration algorithm for elastoplasticity using a semi-implicit Euler scheme (omitting the index $n+1$)

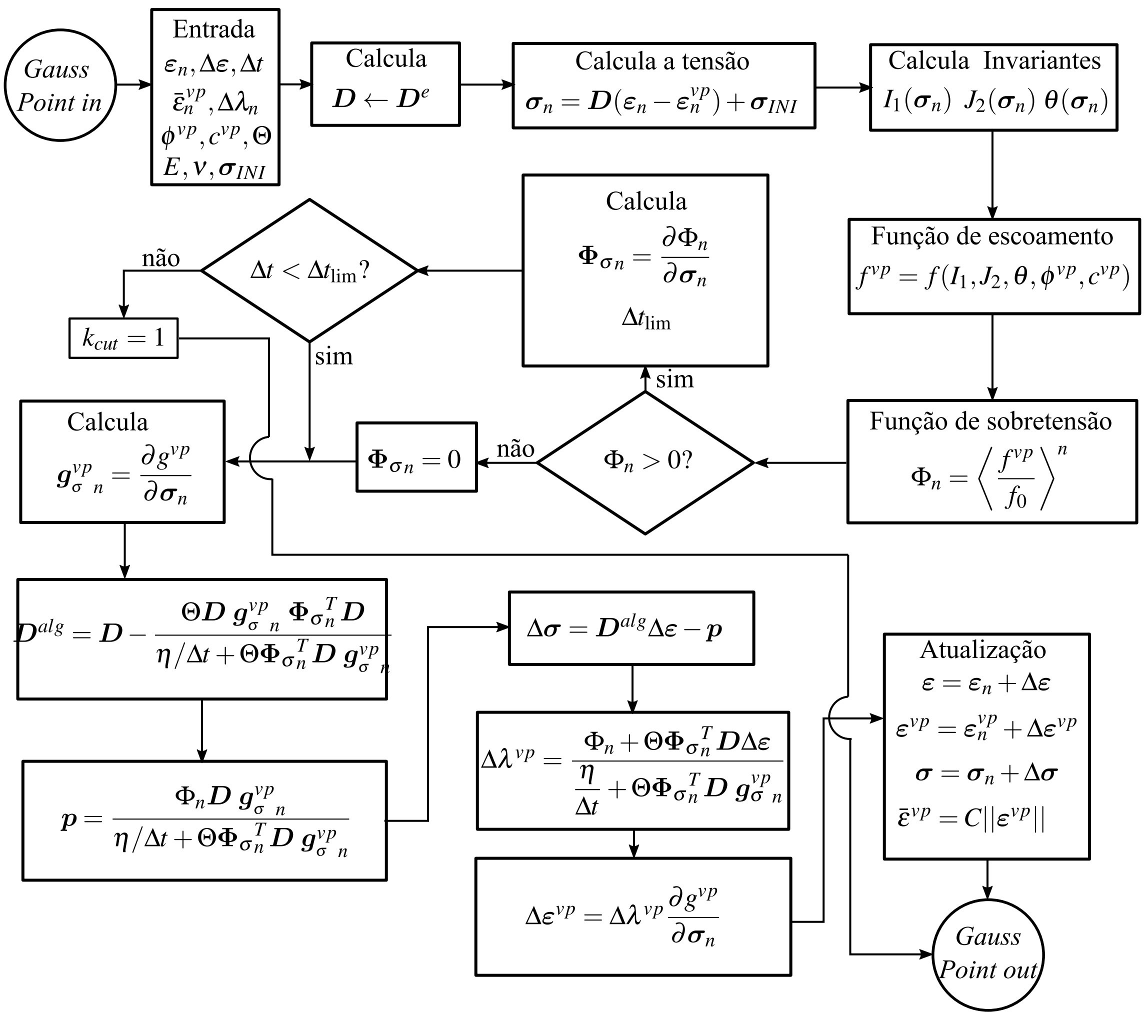

Fig. 6. Integration algorithm for viscoplasticity using a semi-implicit Euler scheme without hardening-softening (omitting the index $n + 1$).

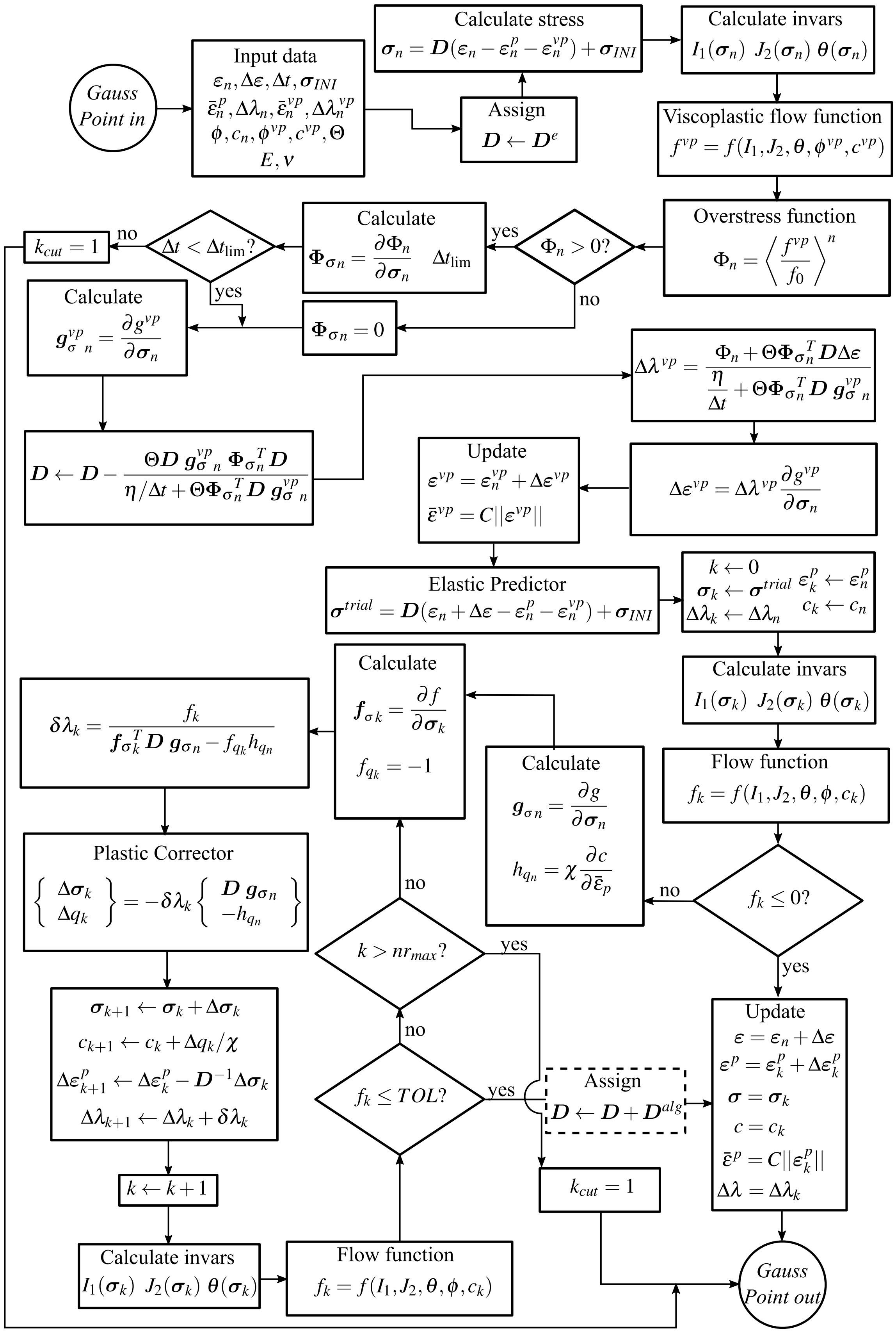

Fig. 7. Integration algorithm for elastoplasticity-viscoplasticity (omitting the index $n + 1$).

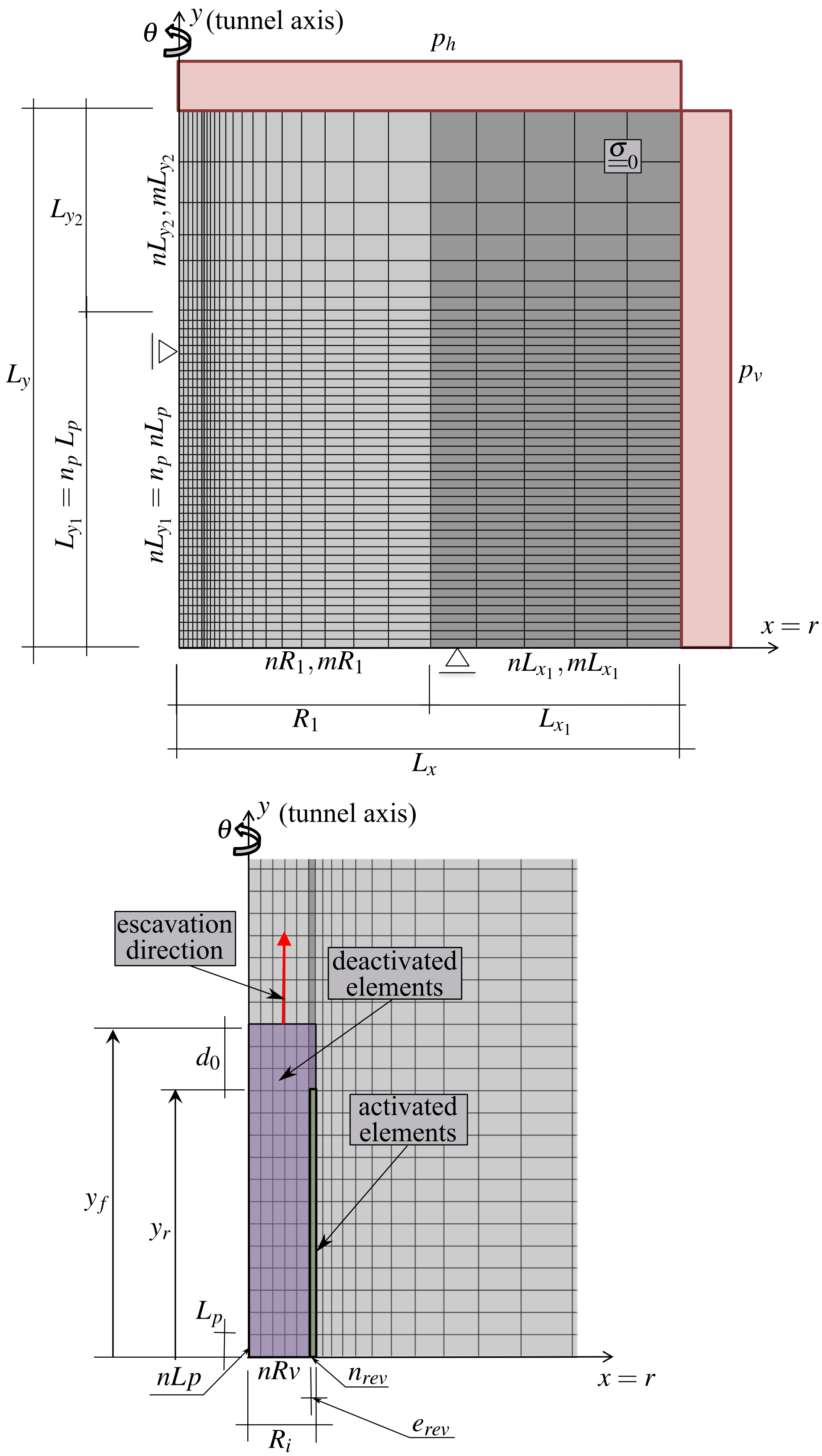

Fig. 8. Domain, parameters, boundary conditions and the mesh of the axisymmetric numerical model.

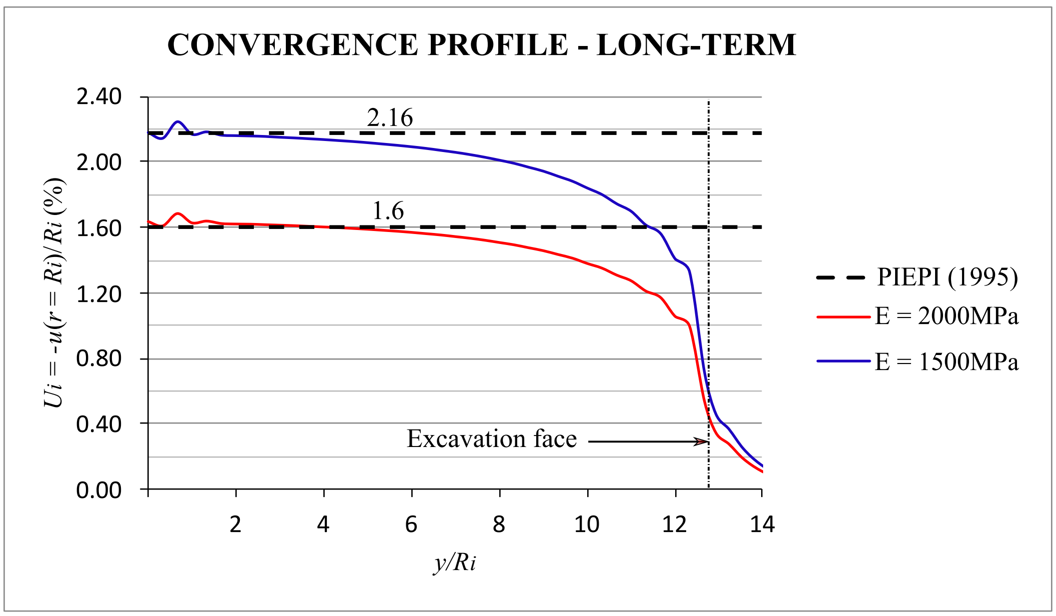

Fig. 9. Verification with Piepi (1995) analytical solution of the model elastoplastic-viscoplastic without lining.

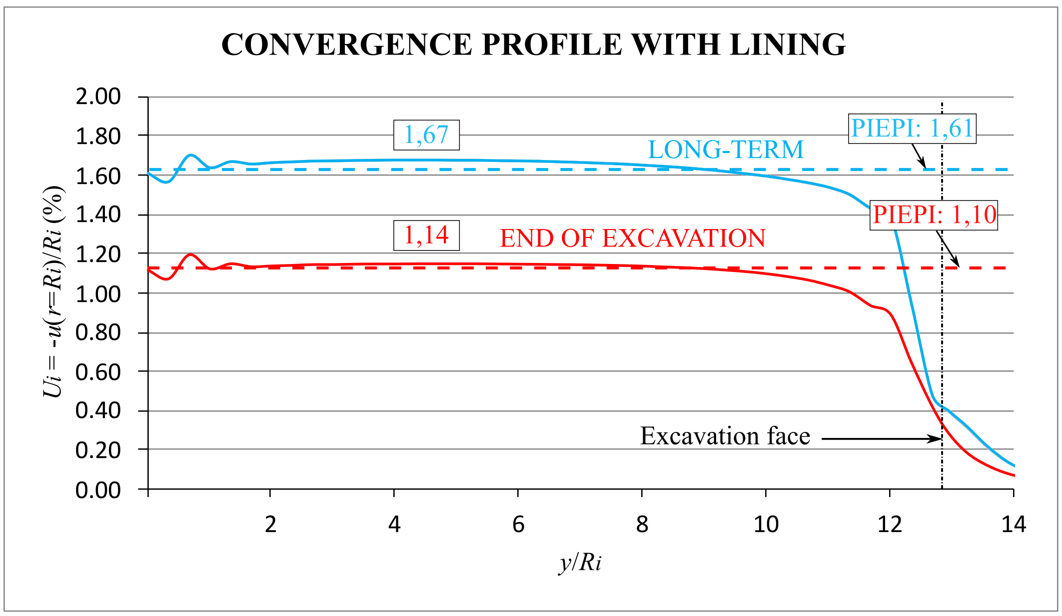

Fig. 10. Verification with Piepi (1995) numerical solution of the model elastoplastic-viscoplastic with lining.

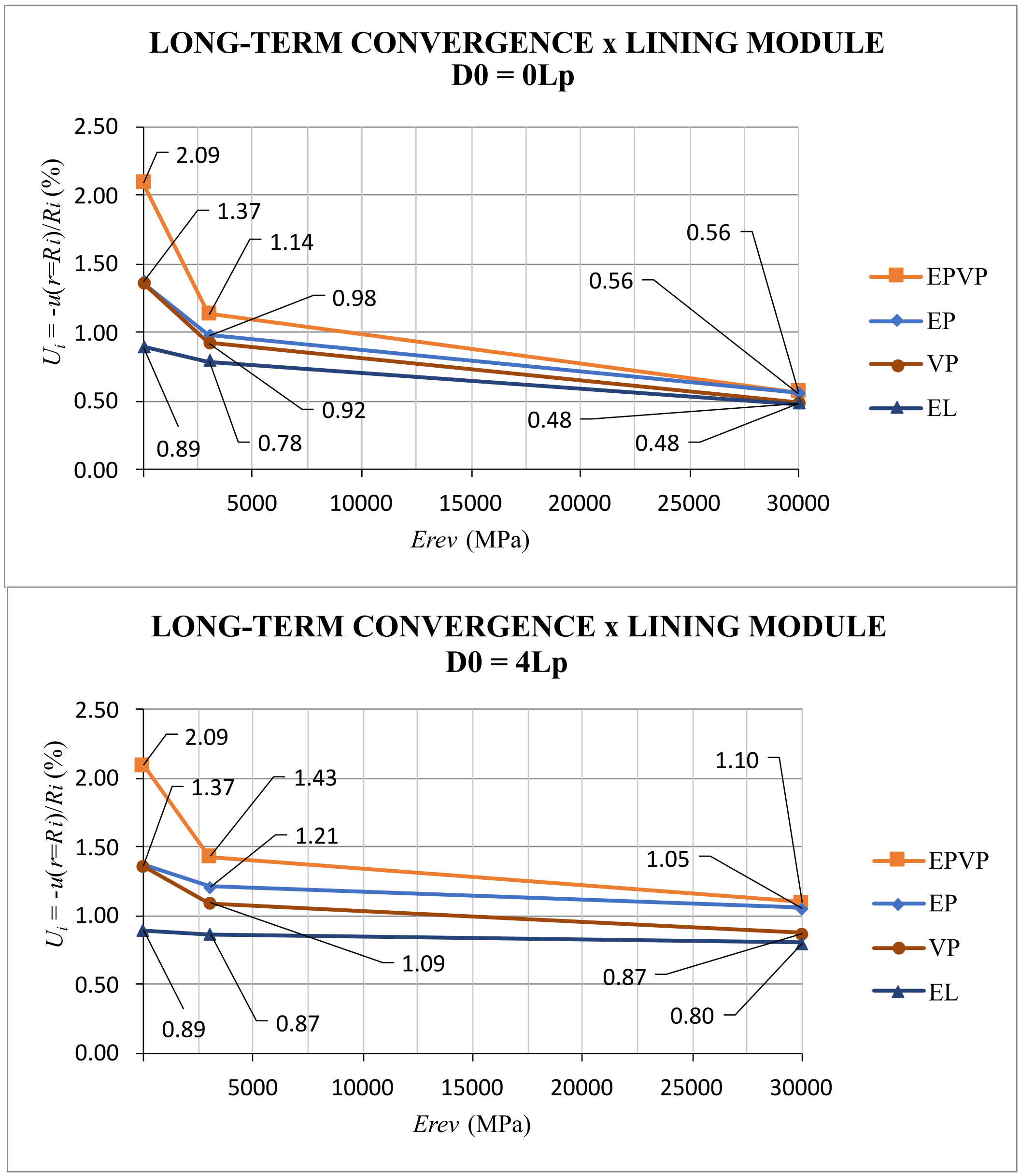

Fig. 11. Long-term convergence versus lining modulus of elasticity for an unsuported distance $d0 = 0$ and $d0 = 4L_p$.